Caderno de Geografia (2026) v.36, Número Especial 2
ISSN 2318-2962
DOI 10.5752/p.2318-2962.2026v36nesp2p129

ORIGINAL ARTICLE

ANALYSIS OF VEGETATION VIGOR IN THE AMAZON BASIN DURING MAJOR DROUGHT EVENTS

Análise do Vigor da Vegetação na Bacia Amazônixa Durante Grandes Eventos de Seca

Pedro Freitas Ramos Grande
Bachelor of Geography, Federal University of Alfenas, Brazil
pfrgrande@gmail.com

Raiane Cristina Pereira
Bachelor of Geography, Brasil
contatoraianepereira@gmail.com

Everton Rodrigues da Silva
PhD in Management, Federal University of Alfenas, Brazil
everton.silva@unifal-mg.edu.br

Marcelo de Oliveira Latuf
PhD in Geography, Federal University of Alfenas, Brazil
marcelo.latuf@unifal-mg.edu.br

Received: 01/02/2026
Accepted: 15/04/2026

Abstract
The Amazon River Basin has experienced an increase in the frequency and intensity of major drought events in the 21st century, driven by climate oscillations and anthropogenic pressures, placing the region at risk of reaching an ecological tipping point. Given this scenario, this study aimed to evaluate the spatiotemporal variability in the impact of major droughts between 2001 and 2024 on the basin's vegetative vigour, using the Enhanced Vegetation Index (EVI) and Modified Normalised Difference Water Index (MNDWI) spectral indices. To this end, time-series processing of the MODIS sensor collections MOD13A3 and MOD09GA was performed on the Google Earth Engine platform, applying dynamic water masks to ensure the accuracy of biomass data. The results indicated that the years 2005, 2010, 2016, and 2024 had the smallest surface water extents in the basin, consistent with El Niño events. It was observed that while the Central Amazon demonstrated greater phenological resilience, the Arc of Deforestation region exhibited severe declines in vegetative vigour during dry periods.

Keywords: Remote Sensing; MODIS; Google Earth Engine; EVI; El Niño.

Resumo
A bacia do rio Amazonas tem enfrentado um aumento na frequência e na intensidade de grandes eventos de seca no século XXI, impulsionados por oscilações climáticas e pressões antropogênicas, o que coloca a região em risco de atingir um ponto de inflexão ecológico. Diante desse cenário, este estudo teve como objetivo avaliar a variabilidade espaço-temporal do impacto de grandes secas ocorridas entre 2001 e 2024 sobre o vigor da vegetação da bacia, utilizando os índices espectrais Índice de Vegetação Aprimorado

ISSN 2318-2962
DOI 10.5752/p.2318-2962.2026v36nesp2p129

(EVI) e Índice de Água por Diferença Normalizada Modificado (MNDWI). Para tanto, foi realizado o processamento de séries temporais das coleções de sensores MODIS MOD13A3 e MOD09GA por meio da plataforma Google Earth Engine, aplicando máscaras de água dinâmicas para garantir a precisão dos dados de biomassa. Os resultados indicaram que os anos de 2005, 2010, 2016 e 2024 registraram as menores extensões de água superficial na bacia, em consonância com a ocorrência de eventos de El Niño. Observou-se que, enquanto a Amazônia Central demonstrou maior resiliência fenológica, a região do Arco do Desmatamento apresentou declínios acentuados no vigor da vegetação durante os períodos de seca.

Palavras-chave: Sensoriamento Remoto; MODIS; Google Earth Engine; EVI; El Niño

1. INTRODUCTION

The river basins of the main Amazonian rivers are among the largest in the world (Latrubesse, 2008). Precipitation seasonality, both in their headwaters and along their courses, conditions the occurrence of well-defined hydrological cycles, characterized by an annual high-water and a low-water season, also referred to as the aquatic and terrestrial phases (Peleja, 2012). However, due to climatic and hydrographic variability, the magnitude of floods and droughts, as well as the average river level amplitude, vary considerably across the different regions of the Amazon Basin (Piedade *et al*., 2013).

Furthermore, several studies point to a correlation between Sea Surface Temperature (SST) anomalies in the Equatorial Pacific (El Niño, La Niña) and the Tropical Atlantic with the basin's rainfall regime (Richey *et al*., 1989; Foley *et al*., 2002; Aalto *et al*., 2003; Ronchail *et al*., 2005; Schöngart; Junk, 2007; Marengo *et al*., 2011). Consequently, several drought events in the Amazon Basin, such as those of 1925/26, 1982/83, and 1997/98, occurred in association with El Niño periods, resulting in reduced flooding and a prolonged terrestrial phase in its floodplain regions (Schöngart *et al*., 2004; Marengo *et al*., 2008).

Although droughts are part of the natural dynamics of the Amazon region, anthropogenic factors such as deforestation, forest degradation, and rising global temperatures have caused an increase in the frequency and intensity of droughts in the Amazon (Coelho *et al*., 2012; Espinoza *et al*., 2024). In this sense, while the last century recorded four extreme droughts, the 21st century has already equaled this total within its first 25 years (Costa *et al*., 2024). The years 2005, 2010, 2015/16, and 2023/24 were marked by historical droughts that progressively surpassed one another, with record maximum temperatures and precipitation below the historical average (Papastefanou *et al*., 2022; Espinoza *et al*., 2024).

ISSN 2318-2962
DOI 10.5752/p.2318-2962.2026v36nesp2p129

These events impact the provision of essential resources for the sustenance of Indigenous Peoples and Local Communities (IPLCs), who depend on the forest's integrity to meet their basic needs, such as food, fibers, and oils (Shanley; Luz, 2003). Furthermore, studies conducted in the Brazilian Amazon indicate that approximately 6 million people in the region rely on the forest and the management of non-timber forest products (NTFPs) for their livelihoods (Lopes *et al*., 2019).

The worsening water deficit and the alteration of hydrological cycles increase the risk of the region crossing a "tipping point," which would result in the irreversible reduction of biological diversity and carbon stocks (Hirota *et al*., 2021). It is estimated that by 2050, between 10% and 47% of the forest could reach this critical threshold, which would tend to exacerbate social inequalities and hinder the consolidation of a socio-bioeconomy based on healthy forests (Flores *et al*., 2024).

The reduction in rainfall during drought periods also influences vegetation, which exhibits high spatial variability. Tree growth in floodable environments is greater during the terrestrial phase (Peleja, 2012), which is prolonged during El Niño events. This condition favors the growth of certain tree species adapted to low-lying floodplains (*low-várzea*), which exhibit significantly wider growth rings in El Niño years (Schöngart *et al*., 2002).

On the other hand, as they are more influenced by precipitation, terra firme forests experience a decrease in photosynthesis rates, increment, and productivity, as well as an increase in mortality during water deficits, potentially becoming carbon sources during these periods (Schöngart *et al*., 2004; Phillips *et al*., 2009). Furthermore, there is an increase in the occurrence of fire events during drought events due to rising air temperatures and the accumulation of fuel load from dry leaf litter and senescent trees (Costa *et al*., 2024).

From a climatic perspective, drought events are defined by insufficient precipitation over a prolonged period or by the temporal inadequacy of rainfall relative to the demands of the vegetation cover (Van Lanen *et al*., 2017). Hydrological drought, in turn, encompasses negative anomalies in surface and subsurface water reserves and is subdivided into streamflow drought, which affects river discharge, and groundwater drought, referring to the lowering of aquifer levels (Van Loon, 2015).

Droughts can be classified according to their severity and the duration of their impacts (Van Lanen *et al*., 2017). For the National Water and Sanitation Agency (ANA), the federal body responsible for regulating the use of water resources in Brazil, droughts lasting less than eight months are considered short-term, while those extending for more than nine months are long-term droughts. Drought intensity is divided into five categories, ranging

ISSN 2318-2962
DOI 10.5752/p.2318-2962.2026v36nesp2p129

from mild drought, which occurs on average every two to five years, to exceptional drought, which occurs once every 50 to 100 years (ANA, 2026).

Given this, there is a substantial need to monitor these phenomena to understand behavioral patterns or correlations between environmental variables that elucidate the intensification of drought profiles in extensive hydrographic regions, as in the case of the Amazon River Basin. In this context, remote sensing has established itself as an indispensable tool for monitoring terrestrial dynamics, allowing for continuous data acquisition across large spatial and temporal scales (Jensen, 2009).

By working with the amount of electromagnetic radiation reflected by terrestrial objects in different spectral bands, remote sensing enables the calculation of spectral indices aimed at monitoring and quantifying vegetation conditions and spatial distribution, based on an understanding of the spectral behavior of targets (Liu, 2015).

Bannari *et al*. (1995) identified more than 40 vegetation indices derived from satellite data developed to analyze the spectral signature of vegetation in remote monitoring. The authors emphasize that this spectral response is modulated by a complex interaction among multiple factors, including vegetation composition, environmental conditions, soil properties, and the spatiotemporal variability of atmospheric conditions.

Among the primary vegetation indices, the Enhanced Vegetation Index (EVI), proposed by Huete *et al*. (1997), represents an advancement over the established Normalized Difference Vegetation Index (NDVI) (Rouse *et al*., 1973), as it was designed to correct distortions caused by soil background signals and atmospheric conditions (Karkauskaite; Tagesson; Fensholt, 2017). According to Didan and Munoz (2019), EVI exhibits greater sensitivity in high-biomass regions by better differentiating soil and vegetation through the decoupling of the canopy background signal, while also experiencing less atmospheric interference.

The EVI calculation incorporates the nonlinear relationship between surface reflectance and vegetation density, in addition to utilizing the blue light band along with the red and near-infrared (NIR) bands already used in the NDVI. This results in more robust values for analyzing vegetation health and vigor, especially in environments with high atmospheric interference (Jaafar *et al*., 2015). Consequently, various studies have found higher accuracy in EVI compared to NDVI regarding seasonal vegetation patterns (Huete *et al*., 2002; Novo *et al*., 2005; Galvão *et al*., 2013; Rosa *et al*., 2013; Melo *et al*., 2024).

In view of this, the objective of this study was to evaluate the spatiotemporal variability of the impact of major 21st-century droughts on the vegetative vigor of the Amazon River

ISSN 2318-2962
DOI 10.5752/p.2318-2962.2026v36nesp2p129

Basin using the Enhanced Vegetation Index (EVI) and Modified Normalized Difference Water Index (MNDWI) spectral indices derived from MODIS products.

2. MATERIALS AND METHODS

To conduct this study, cloud computing techniques were employed, involving both vector and raster spatial data. Figure 1 presents the methodological flowchart implemented:

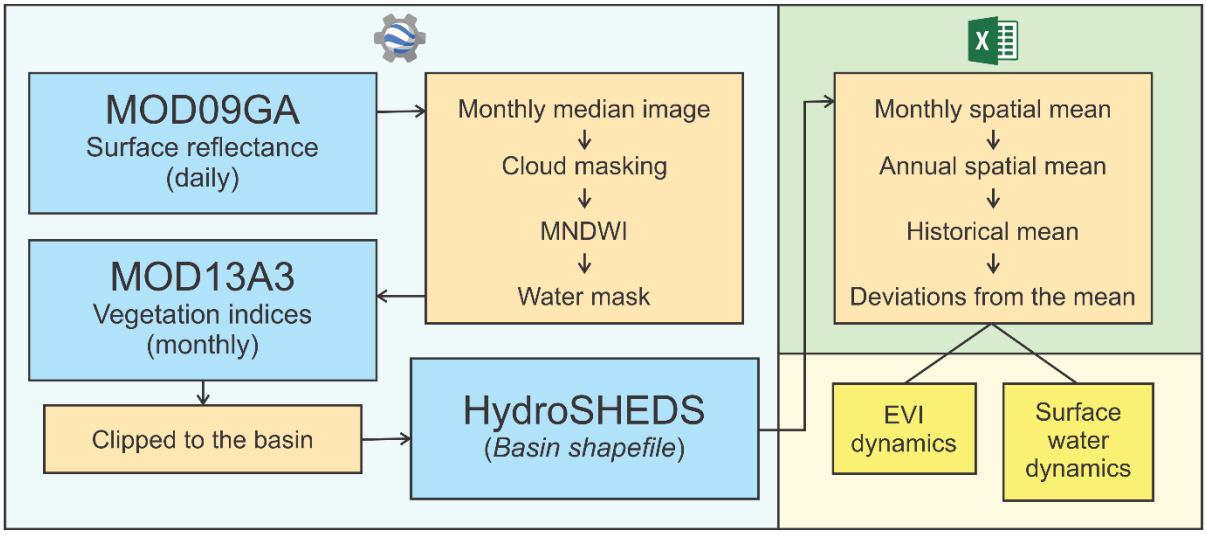

Figure 1 - Methodological flowchart.

The vector data comprised the watershed shapefile provided by the HydroSHEDS platform (Lehner; Grill, 2013) at the following URL: https://www.hydrosheds.org/products/hydrobasins, from which the Amazon River Basin polygon was extracted. Additionally, boundaries for South American countries and Brazilian federative units (states) were used, both acquired from the Metadata Catalog of the National Water and Sanitation Agency (ANA), available at https://www.metadados.snirh.gov.br/.

The raster data consisted of the MOD13A3 v. 6.1 and MOD09GA v. 6.1 collections from the Moderate-Resolution Imaging Spectroradiometer (MODIS), which provide monthly vegetation index products and daily surface reflectance, respectively. All collection processing was performed on the Google Earth Engine cloud platform, which enables the processing of large-scale data volumes via JavaScript programming in the Code Editor API (Gorelick *et al*., 2017).

Initially, it was necessary to standardize the temporal and spatial resolutions of the raster data, given that the MOD13A3 products are provided monthly with a resolution of 1,000 x 1,000 meters per cell, while the MOD09GA data are daily and have bands with 500 x 500-meter cells. To achieve this, the monthly median of the MOD09GA reflectance data

ISSN 2318-2962
DOI 10.5752/p.2318-2962.2026v36nesp2p129

was calculated, and the cells were resampled to 1,000 x 1,000 meters based on the mean of all original grid pixels that overlapped the new pixel.

Regarding the MODIS vegetation index products, the MOD13A3 collection includes the Normalized Difference Vegetation Index (NDVI) (Rouse *et al*., 1973) and the Enhanced Vegetation Index (EVI) (Huete *et al*., 1997). Given the characteristics of the study area, the EVI was selected for this study. The EVI calculation is defined by Equation 1:

$$EVI = G \frac{NIR - Red}{NIR + C1 \times Red - C2 \times Blue + L} \qquad (1)$$

Where NIR, Red, and Blue represent the surface reflectance for the near-infrared, red, and blue bands, respectively; G is the gain factor; C1 and C2 are the aerosol resistance coefficients; and L is the canopy background adjustment. The coefficients adopted for the MODIS MOD13A3 EVI algorithm are: G = 2.5, C1 = 6, C2 = 7.5, and L = 1.

Given the high absorption of electromagnetic radiation by water bodies, which can lead to the underestimation of average EVI values, it was necessary to generate a water mask for each monthly image. To this end, for each monthly median image generated from the MOD09GA collection, a cloud mask was applied using the 'state_1km' band, and the Modified Normalized Difference Water Index (MNDWI), proposed by Xu (2006), was calculated using bands 4 (545–565 nm) and 6 (1,628–1,652 nm).

Thus, potentially flooded areas were excluded from the EVI analysis, and their monthly average areas were quantified. It is important to note that the dynamic water mask was employed solely for calculating the basin's monthly average EVI values and was not applied to the rasters that generated the cartographic products of this study.

The pre-processed database consisted of a time series of 288 monthly EVI images, covering the 24-year analysis period (2001–2024). From this series, annual averages, long-term monthly averages, and an overall mean for the entire period were generated. To evaluate oscillations in the vegetative vigor of the Amazon River Basin, annual EVI deviations were calculated by subtracting the overall historical mean from the mean of the major drought years of this century.

Monthly spatial averages of EVI and surface water area were exported and processed in a spreadsheet environment, where tables and charts were generated. QGIS software version 3.34.2-Prizren was used for the development of the thematic maps.

Caderno de Geografia (2026) v.36, Número Especial 2
ISSN 2318-2962
DOI 10.5752/p.2318-2962.2026v36nesp2p129

3. RESULTS AND DISCUSSION

Since the early 21st century, the Amazon River Basin has been influenced by at least four El Niño phenomena, occurring in the years 2002/03, 2006/07, 2009/10, 2015/16, and 2023/24 (CPTEC, 2024; Peng *et al*., 2025). Between 2001 and 2024, the mapped surface water area of the basin exhibited minima consistent with the major recent droughts documented in the literature (Borma; Nobre, 2013). The years 2005, 2010, 2016, and 2024 showed the lowest mean surface water area values in the basin (Figure 2).

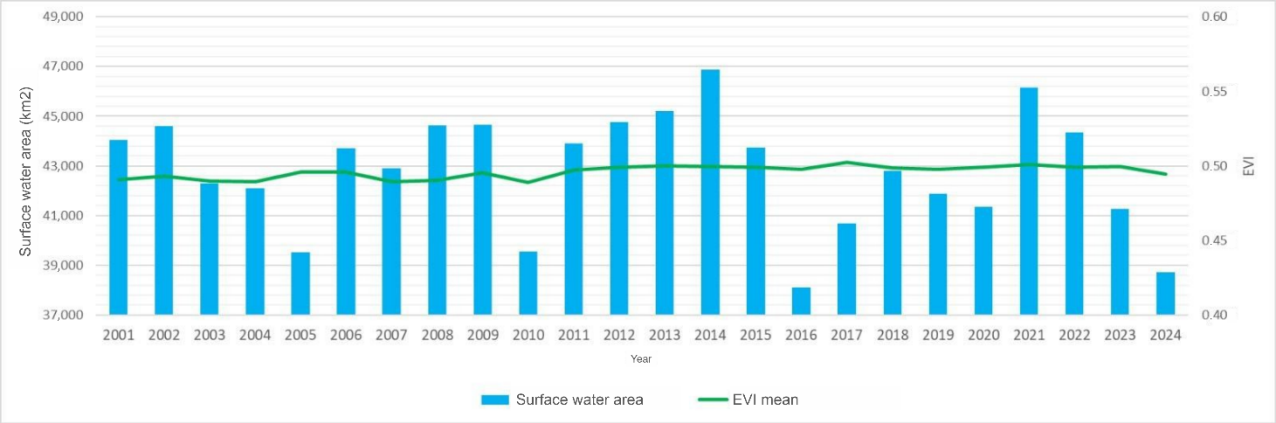

Figure 2 - Annual dynamics of mean EVI and surface water area in the Amazon River Basin (2001–2024).

Coelho *et al*. (2013) demonstrate that the drought events observed in 2005 and 2010 were caused by SST anomalies in the Equatorial Pacific and the Tropical North Atlantic, with the latter reaching the highest recorded SST values in 2010. Gatti *et al*. (2023) evaluated the carbon balance in the Amazon between 2010 and 2020 and pointed to extreme carbon emissions in the region during the 2015 and 2016 El Niño.

Between 2001 and 2024, the study area obtained a mean EVI of 0.496, reaching its maximum annual mean in 2017 and its minimum in 2010, with values of 0.502 and 0.489, respectively. The uniformity of the annual EVI means, observed by the standard deviation of 0.004 and presented in the graph in Figure 2, may mislead toward a simplistic interpretation of the basin's reality, in which vegetation dynamics would supposedly not be affected by fluctuations in water availability.

In this sense, reducing the vegetation behavior of the basin to an annual spatial average is insufficient to identify critical drought periods due to its vast extent, which, besides varying spatially with different hydrological and climatic dynamics, also exhibits temporal variability throughout the annual cycle.

Caderno de Geografia (2026) v.36, Número Especial 2
ISSN 2318-2962
DOI 10.5752/p.2318-2962.2026v36nesp2p129

When evaluating the long-term monthly average of the basin's surface water area (Figure 3), an increase in the water surface is observed between February and May, with a decrease from June to October. Junk *et al*. (1989) defined this water oscillation in two phases: the high-water or aquatic phase and the low-water or terrestrial phase. This flood cycle is of great importance to Amazonian vegetation, as it plays a key role in nutrient cycling and water storage (Piedade *et al*., 2013).

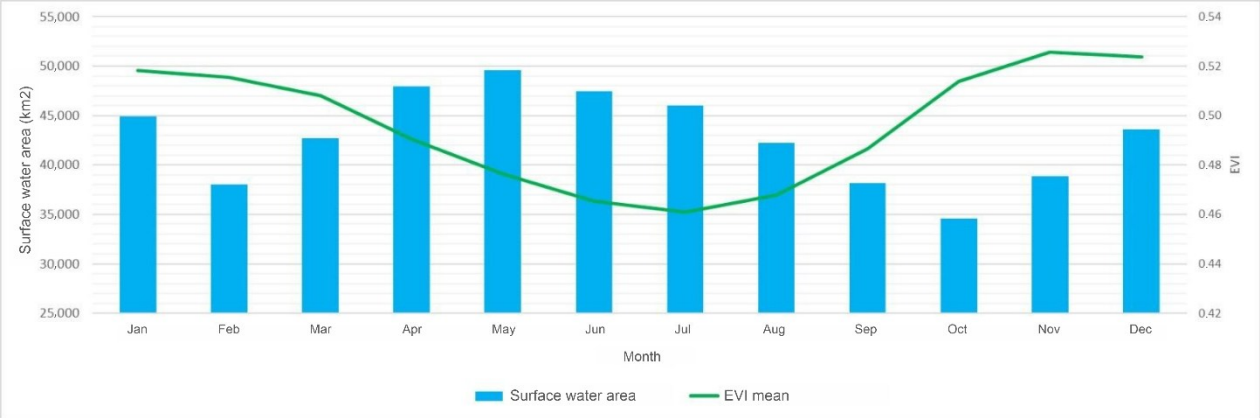

Figure 3 - Monthly dynamics of mean EVI and surface water area in the Amazon River Basin (2001–2024).

The obtained data indicate a decrease in the mean EVI value during the aquatic phase and an increase in the index as the flooded area recedes. This behavior corroborates studies on Amazonian vegetation phenology, which show that different species shed their leaves during the aquatic phase, while others rely on the dry season for their development (Schöngart *et al*., 2002; Parolin *et al*., 2010).

During the flood phase, trees face conditions of hypoxia or anoxia in the root system due to soil saturation (Piedade *et al*., 2013). To circumvent this situation, many species have developed morphological and physiological adaptations, such as the production of adventitious and stilt roots, increased tissue porosity for aerenchyma formation, and the capacity for anaerobic metabolism (Ferreira *et al*., 2010). The cambial activity of many species enters a state of dormancy during flooding, resulting in partial or total leaf loss to reduce water loss, as root absorption is hindered (Horna *et al*., 2002; Piedade *et al*., 2013).

Given the vast and diverse scope of the Amazon River Basin, the spatialization of the variables presented here is fundamental. Based on Figure 4, a decrease in mean EVI values is observed between June and September in the southeastern region of the basin, known as the Arc of Deforestation.

Caderno de Geografia (2026) v.36, Número Especial 2
ISSN 2318-2962
DOI 10.5752/p.2318-2962.2026v36nesp2p129

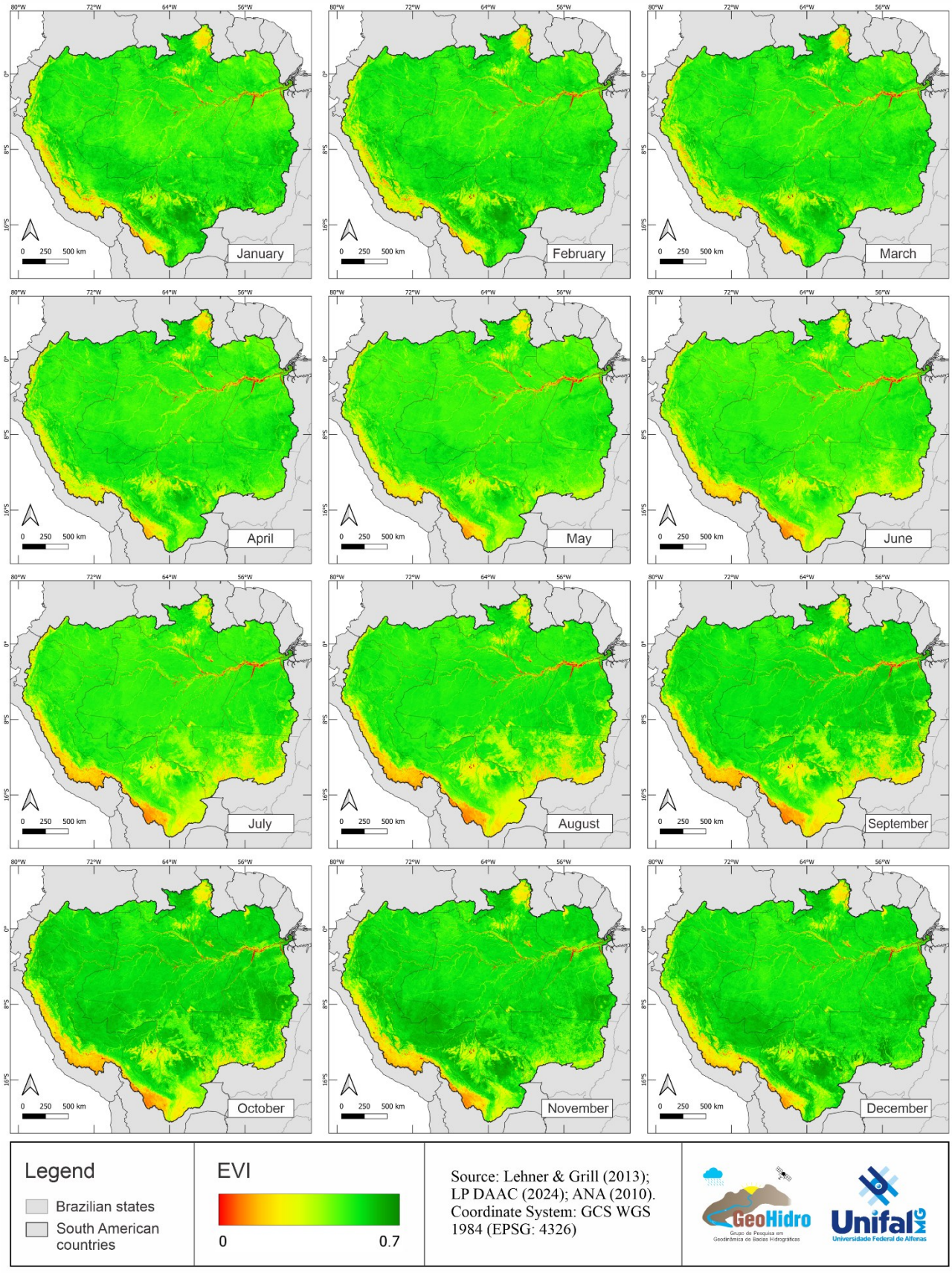

Figure 4 - Monthly mean Enhanced Vegetation Index (EVI) in the Amazon River Basin (2001–2024).

Caderno de Geografia (2026) v.36, Número Especial 2
ISSN 2318-2962
DOI 10.5752/p.2318-2962.2026v36nesp2p129

Conversely, forest formations in the Central Amazon proved to be more resilient than those under anthropogenic pressure, sustaining high EVI values even during dry spells. In this regard, Parolin *et al*. (2010) note that these species exhibit a set of adaptive strategies that enable them to survive the conditions imposed by both flood and drought periods.

The analysis of the spatial dynamics of severe droughts in the Amazon Basin over the past two decades reveals a pattern of increasing intensity and a notable geographical variation in their impacts on vegetation vigor (Figure 5). The 2005 event (Figure 5a), for example, concentrated its most prominent effects in the eastern portion of the Brazilian Amazon and significantly affected the Xingu and Araguaia river basins.

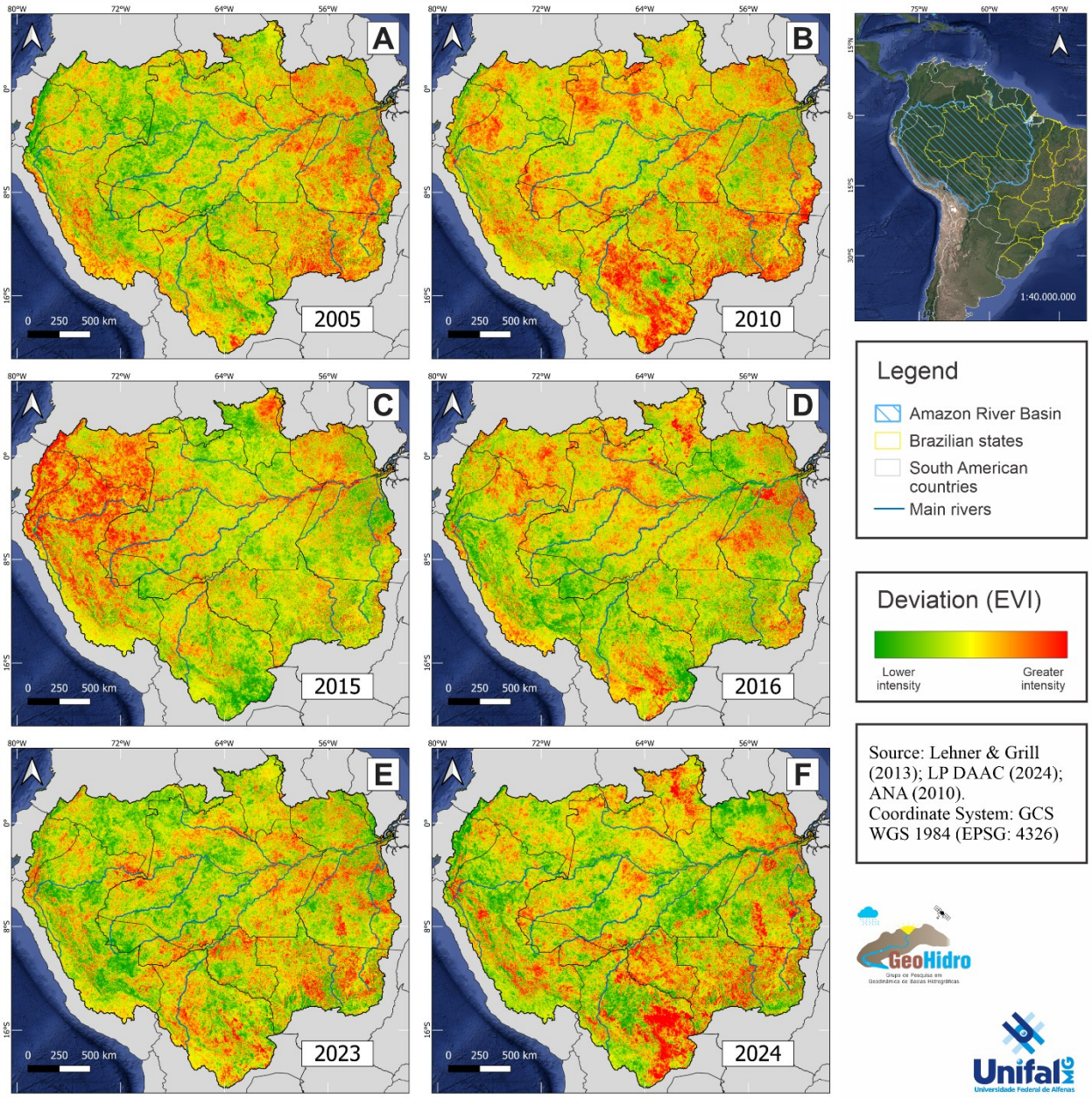

Figure 5 - Impact of major 21st-century droughts on the vegetative vigor of the Amazon River Basin.

ISSN 2318-2962
DOI 10.5752/p.2318-2962.2026v36nesp2p129

Subsequent events suggest an intensification of drought severity in certain locations and demonstrate the recurrence of the phenomenon in specific areas. Regions in Bolivia, for instance, were repeatedly impacted during the droughts of 2010, 2016, 2023, and 2024. However, each event exhibited a distinct spatial signature. Costa *et al*. (2024) point out that during El Niño years, rivers with headwaters in the Northern Hemisphere are more affected by drought due to the concomitance of these events with the natural low-water period, as observed in 2009/10 and 2015/16.

The 2015 (Figure 5c) drought was notable for its expansion toward the westernmost basins, where the impact on vegetation significantly advanced into the upper reaches of the basin. In contrast, in 2016 (Figure 5d) and 2024 (Figure 5f), the degradation of vegetative vigor became particularly evident in the Santarém region. Additionally, the recurrence of dry spells is observed in the Arc of Deforestation, which was affected in 2005, 2010, 2023, and 2024.

The primary triggers for Amazonian droughts are the anomalous warming of the Equatorial Pacific waters, associated with El Niño events, and the Tropical North Atlantic (Coelho *et al*., 2013). The mechanism behind this phenomenon involves the displacement of the descending limb of the Walker Cell over the Amazon, which inhibits cloud formation and reduces precipitation (Williams *et al*., 2005).

In this sense, the warming of the Tropical North Atlantic (TNA) is identified as the primary driver of the 2005 (Figure 5a) and 2010 (Figure 5b) droughts (Tomasella *et al*., 2010). This evolution of impact patterns demonstrates that major droughts in the Amazon are not homogeneous events, but rather phenomena characterized by high geographical variability.

Lian *et al*. (2023) point out that the heat accumulation in the equatorial Pacific Ocean during the winter of 2022 was the highest in the last 40 years, a condition sufficient to trigger a strong El Niño event in late 2023 and early 2024. As observed, the impact of the drought on vegetation was greater in 2024 (Figure 5f) compared to 2023 (Figure 5e). This occurs due to the response time between two distinct hydrological regimes within the same basin, where a time lag of up to four months can be verified for headwaters to reach downstream regions (Schöngart *et al*., 2010).

ISSN 2318-2962
DOI 10.5752/p.2318-2962.2026v36nesp2p129

4. CONCLUSION

This study evaluated the spatiotemporal variability of the impact of major 21st-century droughts on the vegetative vigor of the Amazon River Basin, using the EVI vegetation index as the primary indicator. The results demonstrated that an analysis based on historical mean values for the entire basin, while useful for a general overview, is insufficient and can lead to simplistic interpretations that mask the complex reality of the region. Therefore, the necessity of spatially distributing the processed information became evident to adequately understand vegetation dynamics across such a vast and diverse area.

The importance of this spatial approach was corroborated by the high geographical variability of the impacts observed during different drought events. This study aligns with recent literature on extreme climate events in the Amazon by revealing that each drought has a distinct extent and by identifying the recurrence of dry spells in specific areas, such as the Arc of Deforestation, as well as the greater resilience of Central Amazon forest formations compared to areas under anthropogenic pressure. Consequently, the impact of droughts on Amazonian vegetation comprises a mosaic of distinct responses conditioned by the broad climatic and hydrological variability that characterizes the basin. 2-Prizren was used for the development of the thematic maps.

ACKNOWLEDGEMENTS

The authors would like to thank the National Council for Scientific and Technological Development (CNPq) for the Master's scholarship awarded to the first author of this research.

REFERENCES

AALTO, R.; WOODS, T. N.; DUNNE, T.; LAUER, J. W.; NITTROUER, C. A. Episodic sediment accumulation on Amazonian floodplains influenced by El Niño/Southern Oscillation. **Nature**, London, v. 425, p. 493-497, 2003.

ANA - AGÊNCIA NACIONAL DE ÁGUAS E SANEAMENTO BÁSICO. **Tabela de Classificação de Severidade da Seca**. Brasília, DF: ANA, 2026. Available at: https://monitordesecas.ana.gov.br/tabela-de-classificacao. Accessed on: 20 mar. 2026.

BANNARI, A.; MORIN, D.; BONN, F.; HUETE, A. R. A review of vegetation indices. **Remote Sensing Reviews**, New York, v. 13, n. 1-2, p. 95-120, 1995.

BORMA, L. S.; NOBRE, C. A. (org.). **Secas na Amazônia**: causas e consequências. São Paulo: Oficina de Textos, 2013. 367p

COELHO, C. A. S.; CAVALCANTI, I. A. F.; COSTA, S. M. S.; FREITAS, S. R.; ITO, E. R.; LUZ, G.; SANTOS, A. F.; NOBRE, C. A.; MARENGO, J. A.; PEZZA, A. B. Climate diagnostics of three major drought events in the Amazon and illustrations of their seasonal precipitation predictions. **Meteorological Applications**, Reading, v. 19, n. 2, p. 237-255, 2012.

COELHO, C. A. S.; CAVALCANTI, I. F. A.; ITO, E. R.; SANTOS, A. F.; NOBRE, C. A.; MARENGO, J. A.; PEZZA, A. B. As secas de 1998, 2005 e 2010: análise climatológica. In: BORMA, L. S.; NOBRE, C. A. (org.). **Secas na Amazônia**: causas e consequências. São Paulo: Oficina de Textos, 2013.

COSTA, F. R. C.; MARENGO, J. A.; ALBERNAZ, A. L.; M.; CUNHA, A. P.; CUVI, N.; ESPINOZA, J. C.; FERREIRA, J.; FLEISCMANN, A. S.; JIMENEZ-MUÑOZ, J. C.; PÁEZ, M. B.; QUERIDO, L. C. A.; SCHONGART, J. **Droughts in the Amazon**. Nova Iorque: Science Panel for the Amazon (SPA), 2024. 24p. (Science Panel for the Amazon Policy Brief).

CPTEC - CENTRO DE PREVISÃO DE TEMPO E ESTUDOS CLIMÁTICOS. **El Niño e La Niña**. [S. l.]: INPE, [s. d.]. Available at: http://enos.cptec.inpe.br/. Accessed on: 4 set. 2025.

ESPINOZA, J. C.; JIMENEZ, J. C.; MARENGO, J. A.; SCHONGART, J.; RONCHAIL, J.; LAVADO-CASIMIRO, W.; RIBEIRO, J. V. M. The new record of drought and warmth in the Amazon in 2023 related to regional and global climatic features. **Scientific Reports**, London, v. 14, n. 1, p. 8107, 2024.

FERREIRA, C. S.; FIGUEIRA, A. V. O.; GRIBEL, R.; WITTMANN, F.; PIEDADE, M. T. F. Genetic variability, divergence and speciation in trees of periodically flooded forests of the Amazon: a case study of Himatanthus sucuuba (SPRUCE) Woodson. In: JUNK, W. J.; PIEDADE, M. T. F.; WITTMANN, F.; SCHONGART, J.; PAROLIN, P. (eds.). **Central Amazonian floodplain forests**: ecophysiology, biodiversity and sustainable management. Dordrecht: Springer, 2010. p. 301-312.

FLORES, B. M.; MONTOYA, E.; SAKSCHEWSKI, B.; NASCIMENTO, N.; STAAAL, A.; BETTS, R. A.; LEVIS, C.; LAPOLA, D. M.; ESQUIVEL-MUELBERT, A.; JAKOB, C.; NOBRE, C. A. Critical transitions in the Amazon forest system. **Nature**, London, v. 626, p. 555-564, 2024.

FOLEY, J. A.; BOTTA, A.; COE, M. T.; COSTA, M. H. El Niño-Southern Oscillation and the climate, ecosystems and rivers of Amazonia. **Global Biogeochemical Cycles**, Washington, v. 16, n. 4, p. 1132, 2002.

GALVÃO, L. S.; BREUNIG, F. M.; SANTOS, J. R.; MOURA, Y. M. View illumination effects on hyperspectral vegetation indices in the Amazonian tropical forest. **International Journal of Applied Earth Observation and Geoinformation**, Amsterdam, v. 21, p. 291-300, 2013.

GATTI, L. V.; CASSOL, H. L. G.; MILLER, J. B.; GLOOR, M. E.; DOMINGUES, L. G.; CRISPIM, L. S.; NEVES, L.; COLLAITI, G. S. Increased Amazon carbon emissions mainly from decline in law enforcement. **Nature**, London, v. 621, p. 618-623, 2023.

GLOOR, E.; WILSON, C.; CHIPPERFIELD, M. P.; HOUGHTON, R. A.; PANIZZA COUTO, T. K.; MILLER, J. B. Tropical land carbon cycle responses to 2015/16 El Niño as recorded by atmospheric greenhouse gas and remote sensing data. **Philosophical Transactions of the Royal Society B: Biological Sciences**, London, v. 373, n. 1760, 2018.

GORELICK, N.; HANCHER, M.; DIXON, M.; ILYUSHCHENKO, S.; THAU, D.; MOORE, R. Google Earth Engine: planetary-scale geospatial analysis for everyone. **Remote Sensing of Environment**, New York, v. 202, p. 18-27, 2017.

HIROTA, M.; FLORES, B. M.; BETTS, R.; BORMA, L. S.; ESQUÍVEL-MUELBERT, A.; JAKOVAC, C.; LAPOLA, D. M.; MONTOYA, E.; OLIVEIRA, R. S.; SAKSCHEWSKI, B. Resilience of the Amazon Forest to Global Changes: Assessing the Risk of Tipping Points. In: NOBRE, C. *et al*. (Eds.). **Amazon Assessment Report 2021**. New York: United Nations Sustainable Development Solutions Network, 2021. cap. 24. Disponível em: https://www.theamazonwewant.org/spa-reports/. Acesso em: 23 mar. 2026.

HORNA, V. **Carbon release from woody parts of trees from a seasonally flooded Amazon forest near Manaus**. 2002. 137 f. Tese (Doutorado em Ecologia) – Universidade de Bayreuth, Bayreuth, 2002.

HUETE, A. R.; DIDAN, K.; MIURA, T.; RODRIGUEZ, E. P.; GAO, X.; FERREIRA, L. G. Overview of the radiometric and biophysical performance of the MODIS vegetation indices. **Remote Sensing of Environment**, New York, v. 83, n. 1-2, p. 195-213, 2002.

HUETE, A. R.; LIU, H. Q.; BATCHILY, K.; VAN LEEUWEN, W. A comparison of vegetation indices over a global set of TM images for EOS-MODIS. **Remote Sensing of Environment**, New York, v. 59, p. 440-451, 1997.

JAAFAR, H. H.; MOURAD, R.; SCHILLER, S.; SANTANELLO, J. A. Impact of the Syrian conflict on irrigated agriculture in the Orontes basin. **International Journal of Water Resources Development**, Abingdon, v. 31, n. 4, p. 436-449, 2015.

JENSEN, J. R. **Sensoriamento remoto do ambiente**: uma perspectiva em recursos terrestres. São José dos Campos: Parêntese, 2009. 598p.

JUNK, W. J. Flood tolerance and tree distribution in central Amazonian floodplains. In: HOLM-NIELSEN, L. B.; NIELSEN, I. C.; BALSLEV, H. (ed.). **Tropical forests**: botanical dynamics, speciation and diversity. New York: Academic Press, 1989. p. 47-64.

KARKAUSKAITE, P.; TAGESSON, T.; FENSHOLT, R. Evaluation of the Plant Phenology Index (PPI), NDVI and EVI for start-of-season trend analysis of the northern hemisphere boreal zone. **Remote Sensing**, Basel, v. 9, n. 5, p. 485, 2017.

LATRUBESSE, E. M. Patterns of anabranching channels: the ultimate end-member adjustment of mega rivers. **Geomorphology**, Amsterdam, v. 101, n. 1-2, p. 130-145, 2008.

LEHNER, B.; GRILL, G. Global river hydrography and network routing: baseline data and new approaches to study the world's large river systems. **Hydrological Processes**, Chichester, v. 27, n. 15, p. 2171-2186, 2013.

LIAN, T.; YING, J.; TAN, X.; CHEN, D. A strong 2023/24 El Niño is staged by tropical Pacific Ocean heat content buildup. **Ocean-Land-Atmosphere Research**, Washington, v. 2, n. 0011, 2023.

LIU, W. T. H. **Aplicações de sensoriamento remoto**. São Paulo: Oficina de Textos, 2015. 102p.

LOPES, E.; DE CARVALHO, R. L.; GIMENEZ, B.; LOPES, A.; BARBOSA, A. Mapping the socio-ecology of non timber forest products (NTFP) extraction in the Brazilian Amazon: the case of açaí (Euterpe precatoria Mart) in Acre. **Landscape and Urban Planning**, Amsterdam, v. 188, p. 110-117, 2019.

MARENGO, J. A.; NOBRE, C. A.; TOMASELLA, J.; OYAMA, M. D.; OLIVEIRA, G. S.; OLIVEIRA, R.; CAMARGO, H.; ALVES, L. M.; BROWN, I. F. The drought of Amazonia in 2005. **Journal of Climate**, Boston, v. 21, n. 3, p. 495-516, 2008.

MARENGO, J. A.; TOMASELLA, J.; ALVES, L. M.; SOARES, W. R.; RODRIGUEZ, D. A. The drought of 2010 in the context of historical droughts in the Amazon region. **Geophysical Research Letters**, Washington, v. 38, n. 12, L12703, 2011.

MELO, J. L. M. B.; SILVA, G. H. G.; BANDEIRA, A. J. B.; BRAGA, D. G. F.; PADILHA, J.; SILVA, A. K. M.; VILANOVA, R. S.; DELGADO, R. C. Influência dos eventos climáticos de El Niño e La Niña em uma área de floresta ombrófila aberta na Amazônia ocidental. In: SILVA, B. K. A.; PETERS, L. P.; CARVALHO, C. M. (orgs.). **Ciência, inovação e tecnologia na Amazônia**: rumos para o desenvolvimento sustentável da amazônia. Rio Branco: Stricto Sensu, 2024. p. 7-19.

NOVO, E. M. L. M.; BARBOSA, C. C. F.; FREITAS, R. M.; SHIMABUKURO, Y. E.; MELACK, J. M.; PEREIRA FILHO, W. Técnicas avançadas de sensoriamento remoto aplicadas ao estudo de mudanças climáticas e ao funcionamento dos ecossistemas amazônicos. **Acta Amazonica**, Manaus, v. 35, n. 2, p. 259-272, 2005.

PAPASTEFANOU, P.; ZANG, C. S.; ANGELOV, Z.; DE CASTRO, A. A.; JIMENEZ, J. C.; DE REZENDE, L. F. C.; RUSCICA, R. C.; SAKSCHEWSKI, B.; SÖRENSSON, A. A.; THONICKE, K.; VERA, C.; VIOVY, N.; VON RANDOW, C.; RAMMIG, A. Recent extreme drought events in the Amazon rainforest: assessment of different precipitation and evapotranspiration datasets and drought indicators. **Biogeosciences**, Göttingen, v. 19, n. 16, p. 3843-3861, 2022.

PAROLIN, P.; LUCAS, C.; PIEDADE, M. T.; WITTMANN, F. Drought responses of flood-tolerant trees in Amazonian floodplains. **Annals of Botany**, Oxford, v. 105, n. 1, p. 129-139, 2010.

PELEJA, J. R. P. Interações aquático-florestais. In: PELEJA, J. R. P.; MOURA, J. M. S. **Estudos Integrativos da Amazônia – EIA**. São Paulo: Acquerello, 2012. cap. 7, p. 197-222.

PENG, Q.; XIE, S. P.; MIYAMOTO, A.; DESER, C.; ZHANG, P.; LUONGO, M. T. Strong 2023–2024 El Niño generated by ocean dynamics. **Nature Geoscience**, London, v. 18, p. 471–478, 2025.

PHILLIPS, O. L. *et al*. Drought sensitivity of the Amazon rainforest. **Science**, Washington, v. 323, n. 5919, p. 1344-1347, 2009.

PIEDADE, M. T. F.; *et al*. Impactos ecológicos da inundação e seca na vegetação das áreas alagáveis amazônicas. In: BORMA, L. S.; NOBRE, C. A. (org.). **Secas na Amazônia**: causas e consequências. São Paulo: Oficina de Textos, 2013.

RICHEY, J. E.; NOBRE, C. A.; DESER, C. Amazon river discharge and climate variability: 1903-1985. **Science**, Washington, v. 246, n. 4926, p. 101-104, 1989.

RONCHAIL, J.; *et al*. Discharge variability within the Amazon basin. In: FRANKS, S. *et al*. (ed.). **Regional hydrological impacts of climatic change**: hydroclimatic variability. Wallingford: IAHS Press, 2005. p. 21-30.

ROSA, P. A.; COELHO, G. C.; LOREGIAN, A. C.; GOMES, J. P. Dinâmica da Floresta do Parque Estadual do Turvo com Índices de Vegetação. **Floresta e Ambiente**, Seropédica, v. 20, n. 4, p. 487-499, 2013.

SCHÖNGART, J.; JUNK, W. J. Forecasting the flood-pulse in Central Amazonia by ENSO-indices. **Journal of Hydrology**, Amsterdam, v. 335, n. 1-2, p. 124-132, 2007.

SCHÖNGART, J.; JUNK, W. J.; PIEDADE, M. T. F.; AYRES, J. M.; HÜTTERMANN, A.; WORBES, M. Teleconnection between tree growth in the Amazonian floodplains and the El Niño- Southern Oscillation effect. **Global Change Biology**, Oxford, v. 10, n. 5, p. 683-692, 2004.

SCHÖNGART, J.; PIEDADE, M. T. F.; LUDWIGSHAUSEN, S.; HORNA, V.; WORBES, M. Phenology and stem-growth periodicity of tree species in Amazonian floodplain forests. **Journal of Tropical Ecology**, Cambridge, v. 18, n. 4, p. 581-597, 2002.

SCHÖNGART, J.; WITTMANN, F.; WORBES, M. Biomass and NPP of Central Amazonian floodplain forests. In: JUNK, W. J. *et al*. (ed.). **Central Amazonian floodplain forests**: ecophysiology, biodiversity and sustainable management. Dordrecht: Springer, 2010. cap. 15, p. 347-388.

SHANLEY, P.; LUZ, L. The impacts of forest degradation on medicinal plant use and implications for health care in eastern Amazonia. **Bioscience**, Oxford, v. 53, n. 6, p. 573-584, 2003.

TOMASELLA, J.; BOULANGER, J. P.; AMBROZIO, G.; OLIVEIRA, S. M.; OLIVEIRA, R. P.; BARBOSA, M.; RODRIGUEZ, D. A. The droughts of 1996-1997 and 2004-2005 in Amazonia: hydrological response in the river main-stem. **Hydrological Processes**, Chichester, v. 25, n. 8, p. 1228-1242, 2010.

VAN LANEN, H. A. J.; VOGT, J. V.; ANDREU, J. *et al*. Climatological risk: droughts. In: POLJANŠEK, K.; MARIN FERRER, M.; DE GROEVE, T.; CLARK, I. (Eds.). **Science for Disaster Risk Management 2017**: knowing better and losing less. Luxembourg: Publications Office of the European Union, 2017. p. 271-293.

VAN LOON, A. F. Hydrological drought explained. **WIREs Water**, Hoboken, v. 2, p. 359-392, 2015.

WILLIAMS, E.; SANTOS, A.; SERGIO, L. The drought of the century in the Amazon basin: an analysis of the regional variation of rainfall in South America in 1926. **Acta Amazonica**, Manaus, v. 35, n. 2, p. 231-238, 2005.

XU, H. Modification of normalised difference water index (NDWI) to enhance open water features in remotely sensed imagery. **International Journal of Remote Sensing**, Abingdon, v. 27, n. 14, p. 3025-3033, 2006.

Received: 01/02/2026
Accepted: 15/04/2026